Proceedings of the 21st ICSMGE, Vienna, Austria, 14 – 19 June 2026. Pistrol, Adam & Schweiger (eds.)
Published by: ÖGG, Austrian Society for Geomechanics, Salzburg, Austria, ISBN 978-3-9503898-4-5
https://doi.org/10.53243/ICSMGE2026-162

Experimental and numerical analysis of soil-geogrid composites under road construction stress conditions

Mindaugas Zakarka, Šarūnas Skuodis, Neringa Dirgėlienė
Department of Reinforced Concrete Structures and Geotechnics, Vilnius Gediminas Technical University, Lithuania, mindaugas.zakarka@vilniustech.lt

ABSTRACT: The interaction between soil and geogrid reinforcement is multifaceted and critically influences the mechanical behavior of reinforced ground systems. In numerical modeling, geogrids are typically idealized as tensile elements; however, real interaction mechanisms involve friction, bonding, and interlocking effects, making it more accurate to treat the system as a composite material. This study investigates these interactions through consolidated drained triaxial compression tests conducted on three types of sand, both unreinforced and reinforced with a geogrid, under confining pressures of 20, 50, and 70 kPa—stress conditions representative of road construction subgrades. The laboratory results were used to derive strength and stiffness parameters, which were then applied in PLAXIS 3D using the Hardening Soil model. The model calibration focused on matching axial deformation behavior while retaining peak deviatoric stress consistency. The power index *m* was determined graphically and was found to remain within a similar range for both reinforced and unreinforced conditions. Reinforced samples exhibited higher stiffness and apparent cohesion, confirming the mechanical benefit of geogrid inclusion. The calibrated model demonstrated satisfactory agreement with experimental results, indicating that the Hardening Soil model, when properly calibrated, can represent the behavior of geogrid-reinforced soils. These findings support the further use and development of FEM approaches for reinforced soil systems under low-stress conditions typically encountered in road subgrades.

KEYWORDS: geogrid reinforcement, triaxial compression test, Hardening Soil model, FEM calibration.

1 INTRODUCTION

The use of geosynthetics has become a standard solution in modern geotechnical engineering, especially for improving the performance of road structures constructed over weak or variable subgrades. Among these materials, geogrids are particularly valued for their capacity to enhance load distribution, reduce deformation, and increase the overall stability of soil structures (Rathmayer et al., 2019; Bhardwaj & Mittal, 2022). Geogrids are widely utilized in various infrastructure projects to reduce settlement and enhance mechanical properties of granular soils, thereby increasing the durability and service life of engineered structures (Zornberg, 2017).

One of the key challenges in evaluating geogrid effectiveness lies in understanding the interaction between soil and geogrid under realistic loading scenarios. Laboratory testing methods such as direct shear, pullout, and triaxial compression provide insights into different interaction mechanisms (Palmeira, 2009; Makkar, 2019). These methods are complemented by numerical and analytical simulations that help generalize laboratory findings and improve the optimization of reinforced soil structures (Calvello & Finno, 2004; Ikeagwuani & Nwonu, 2019). Among the laboratory techniques, triaxial tests are particularly well-suited for assessing soil behavior under varied confining pressures, as they enable more representative simulation of field conditions. This is especially relevant in road construction, where confining pressures are typically low (Heerten, 2007).

Finite element modeling (FEM) is commonly used to simulate soil–geogrid systems, with the Hardening Soil model providing a versatile framework for incorporating nonlinearity and stress-dependent stiffness (Brinkgreve, 2013). The Hardening Soil model has demonstrated good agreement with stress–strain behavior in triaxial compression tests (Pacheco et al., 2021), assuming that model parameters are carefully calibrated based on high-quality experimental data. Nonetheless, conventional FEM approaches often simplify geogrids as purely tensile elements, overlooking additional mechanisms such as interlocking and bonding with surrounding soil particles (Skuodis et al., 2020). As a result, they may not fully capture the composite behavior observed in reinforced soil systems.

Recent developments have emphasized the need to model reinforced soil as a unified material with emergent composite properties, particularly when calibrating numerical models based on experimental data (Pham, 2023; Zakarka & Skuodis, 2024). Despite these advancements, parameter selection guidelines – such as those for stiffness modulus and power index *m* – remain primarily focused on unreinforced soils (Rebolledo et al., 2019).

Although progress has been made in understanding reinforced soils, calibrated values for stiffness and compressibility in geogrid-reinforced systems are still limited in practical applications. This study contributes to filling this gap by calibrating geogrid-reinforced sand behavior using triaxial test results and FEM simulations under low confining stress conditions (20–70 kPa) representative of road embankments.

2 MATERIALS AND METHODS

Three types of sand were used in the study and classified according to LST EN ISO 14688-2 (2020) standard as poorly graded sand (SaU) and moderately graded sand (SaM). For simplicity and reference, they are denoted as Soil 1 (SaU), Soil 2 (SaM), and Soil 3 (SaU). Their granulometric properties are summarized in Table 1.

Table 1. Particle size distribution and classification parameters of tested sands.

Soil	Classification	d_{10}	d_{30}	d_{50}	d_{60}	C_U	C_C
1	SaU	0.09	0.15	0.19	0.21	2.25	1.08
2	SaM	0.23	0.44	1.05	2.00	8.17	0.46
3	SaU	0.14	0.20	0.28	0.43	2.45	0.79

For triaxial compression testing, all soil samples were prepared under controlled conditions. To ensure consistency, samples were re-compacted to reach their optimal bulk densities at optimal water contents, as determined by standard Proctor compaction tests according to LST EN ISO 13286-2 (2015). The compaction parameters used for specimen preparation were

previously published in Zakarka et al. (2023) and are summarized in Table 2.

Table 2. Sample preparation parameters.

Soil	w_{opt} (%)	ρ_d (g/cm^3)	ρ (g/cm^3)
1	14.30	1.65	1.86
2	8.80	1.98	2.16
3	8.00	1.75	1.90

A polyester geogrid with a square mesh size of 25 × 25 mm and tensile strength of 40 kN/m was used as reinforcement. The geogrid was trimmed to fit the 100 mm diameter samples, with a slight clearance to prevent edge interference. It was placed horizontally at the mid-height of the specimen during sample preparation. Cylindrical specimens (diameter 100 mm, height 200 mm) were prepared in 10 layers to ensure uniform compaction.

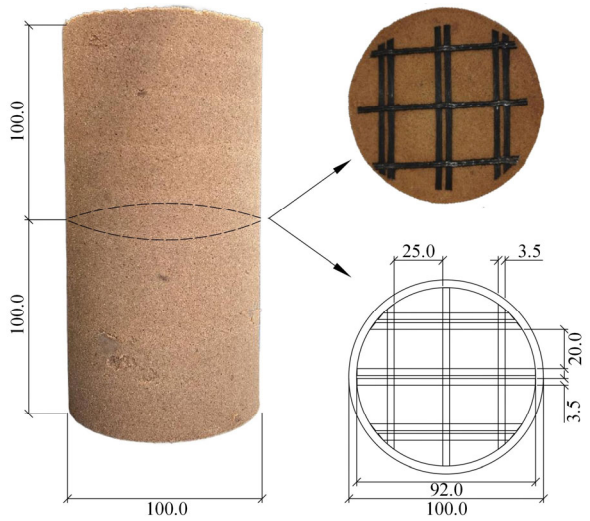

Figure 1. Prepared geogrid-reinforced specimen for the triaxial testing (Zakarka, 2025).

All specimens were subjected to consolidated drained (CD) triaxial compression testing under confining pressures of 20, 50, and 70 kPa. These values reflect stress conditions typically encountered in road embankments and subgrades, and have been identified as representative for simulating road construction loading scenarios (Zakarka, 2022). Testing was conducted in accordance with LST EN ISO 17892-9 (2018), with vertical loading applied at 0.95%/min until 15% axial strain was reached.

The deviatoric stress at failure was used to derive strength parameters c' and φ' based on the Mohr–Coulomb failure criterion. Stiffness parameters – namely the secant stiffness modulus E_{50}, the reference stiffness modulus E_{50}^{ref}, and the power index m – were determined from the experimental results.

These parameters served as input values for numerical modeling in PLAXIS 3D using the SoilTest module with the Hardening Soil model. For the reinforced and unreinforced soil simulations, model calibration was conducted by adjusting E_{ur} and m values to achieve better agreement between measured and simulated axial strain–stress relationships, with a focus on capturing deformation behavior while preserving the strength response. The initial values for E_{oed} and E_{ur} were selected based on standard PLAXIS recommendations: $E_{oed}^{ref} = E_{50}^{ref}$, $E_{ur}^{ref} = 3E_{50}^{ref}$, Poisson's ratio $\nu = 0.3$, and $K_0^{nc} = 1–\sin\varphi$'.

The power inde was determined from experimental stiffness variation using a logarithmic relationship between stiffness modulus and confining pressure, following the methodology proposed by Konyushkov et al. (2023). A regression line was fitted for each soil type under both reinforced and unreinforced conditions. The resulting slope corresponds to the power index m, which describes the stiffness dependency on the confining pressure. This approach allowed consistent evaluation of the stiffness nonlinearity in reinforced soils, accounting for the reinforcement effects on deformation behavior.

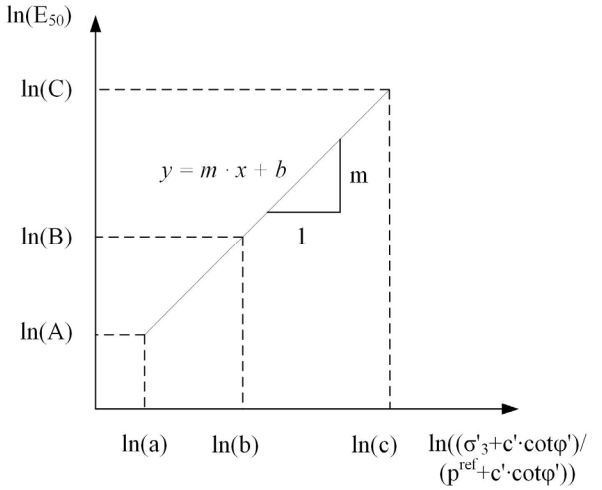

Figure 2. Graphical determination of power index m based on Konyushkov et al. (2023).

3 RESULTS

3.1 *Strength parameters from triaxial tests*

The triaxial compression tests were previously published in Zakarka et al. (2023), where detailed mechanical properties of geogrid-reinforced and unreinforced sands were reported. However, no numerical modelling was performed in the previous work. In this study, those experimentally derived parameters were used for numerical model development and calibration purposes. Triaxial compression tests were conducted on all three sand types under confining pressures of 20, 50, and 70 kPa. Table 3 presents the average effective cohesion (c'_{mean}) and internal friction angle (φ'_{mean}) obtained from the tests. Reinforcement with a geogrid had a limited effect on the friction angle, while a clear increase in cohesion (apparent cohesion) was observed.

Table 3. Average strength parameters of tested soils with and without geogrid reinforcement (Zakarka et al., 2023).

Soil	Condition	φ'_{mean} (°)	c'_{mean} (kPa)
1	Unreinforced	44.24	0.00
	Reinforced	43.98	3.61
	Difference	-0.26	9.31
2	Unreinforced	45.44	0.00
	Reinforced	44.71	9.94
	Difference	-0.73	9.94
3	Unreinforced	43.10	1.81
	Reinforced	42.38	10.65
	Difference	-0.72	8.84

Although the friction angle slightly decreased upon reinforcement, the increased cohesion can be attributed to the interlocking of soil particles within the geogrid apertures and membrane confinement effects. These strength parameters were then used in the numerical model as input values.

3.2 *Stiffness parameters from experimental results*

The stiffness parameters derived from triaxial compression tests included the secant modulus E_{50}, reference stiffness modulus E_{50}^{ref}, and power index m. These parameters were determined at each confining pressure for both unreinforced and reinforced conditions. Table 4 presents the average values used as initial input for numerical simulations.

Table 4. Stiffness parameters from experimental tests.

Soil	Condition	E_{50}^{ref} (kPa)	m
1	Unreinforced	55.99	0.72
	Reinforced	62.08	0.82
2	Unreinforced	43.92	0.68
	Reinforced	54.02	0.94
3	Unreinforced	67.54	0.66
	Reinforced	78.38	0.93

3.3 *Deviatoric stress and deformation matching*

Deviatoric stress values at peak were already reasonably well captured using strength and stiffness parameters derived directly from laboratory results (Figure 3). Slight discrepancies were observed at the lowest confining pressure of 20 kPa, which were expected based on the literature. Therefore, numerical calibration focused primarily on improving the agreement in axial deformation behavior.

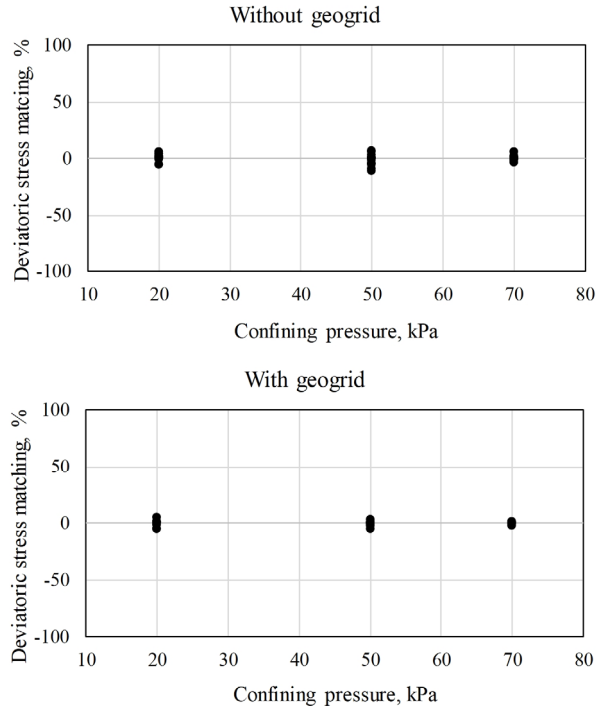

Figure 3. Comparison of deviatoric stress peaks between laboratory tests and numerical modeling.

However, as shown in Figure 4, deformation mismatches reached up to ±50%, especially at the lowest confining pressure (20 kPa), where measurement uncertainty and simplified modeling assumptions had the most impact. To reduce the deviation between laboratory and numerical strain results to within ±10%, calibration was performed by adjusting the values of E_{ur}^{ref} and m.

The final calibrated results, showing improved match between laboratory and modeled deformations, are presented in Figure 5. The corresponding stiffness parameters after calibration are summarized in Table 5.

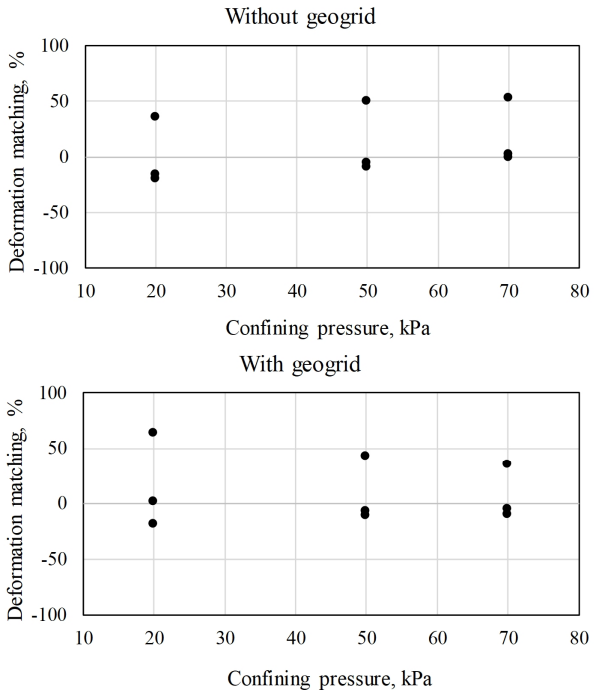

Figure 4. Comparison of vertical deformations between laboratory tests and numerical modeling.

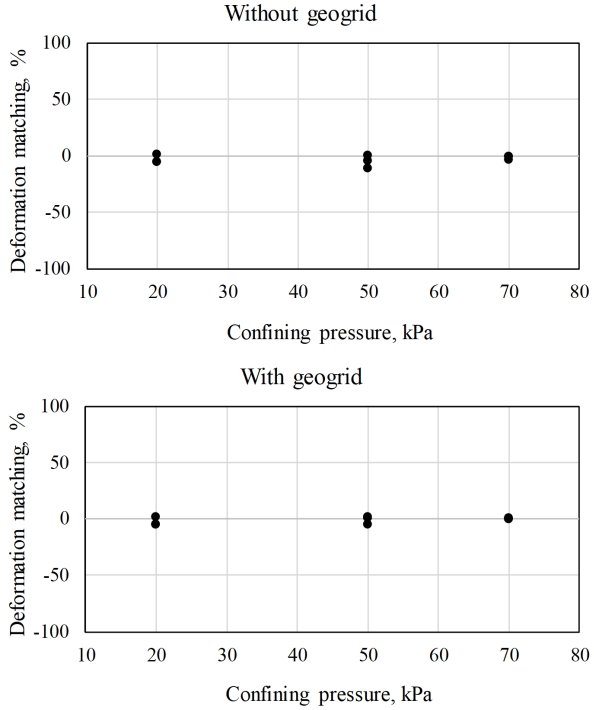

Figure 5. Improved agreement after parameter calibration.

Table 5. Stiffness parameters after numerical calibration.

Soil	Condition	$E_{ur}^{ref}/E_{50}^{ref}$	m
1	Unreinforced	5.00	0.75
	Reinforced	5.00	0.80
2	Unreinforced	11.00	0.80
	Reinforced	11.00	0.80
3	Unreinforced	5.00	0.70
	Reinforced	7.50	0.75

The calibrated values show that reinforced soils generally required higher m values to match observed deformations,

reflecting the stiffening and deformation-limiting effects of geogrid inclusion.

4 CONCLUSIONS

This study investigated the applicability of the Hardening Soil model to simulate the mechanical response of geogrid-reinforced sands under low confining pressures representative of road construction subgrades. Laboratory triaxial compression tests provided strength and stiffness parameters for both unreinforced and reinforced conditions, which served as input for numerical simulations in PLAXIS 3D.

The results showed that peak deviatoric stresses could be reproduced reasonably well using direct laboratory-derived parameters. However, numerical calibration was necessary to improve the match with axial deformation behavior. The reinforced soils exhibited greater stiffness and increased cohesion (apparent cohesion), confirming the effectiveness of geogrid inclusion.

The graphical methodology for determining the power index *m* was successfully applied to both reinforced and unreinforced soils. While reinforcement increased the magnitude of stiffness parameters, the overall stress-dependency (as represented by *m*) remained within a comparable range.

Although the Hardening Soil model proved capable of simulating the composite behavior of geogrid-reinforced sands when calibrated appropriately, further research is warranted. In particular, full-scale and field tests are recommended to validate the general applicability of this modeling approach for practical engineering design.

5 ACKNOWLEDGEMENTS

This research work has received funding from the project „Civil Engineering Research Centre“ (agreement No S-A-UEI-23-5, ŠMSM).

6 REFERENCES

Bhardwaj, A. and Mittal, S., 2022. Influence of Biaxial Geogrid at the Ballast Interface for Granular Earth Railway Embankment. *The Baltic Journal of Road and Bridge Engineering*, 17(3), pp.1–20. https://doi.org/10.7250/bjrbe.2022-17.566.

Brinkgreve, R.B.J., 2013. Validation of geotechnical finite element analysis. 18th International Conference on Soil Mechanics and Geotechnical Engineering. Paris.

Calvello, M. and Finno, R.J., 2004. Selecting parameters to optimize in model calibration by inverse analysis. *Computers and Geotechnics*, 31(5), pp.410–424. https://doi.org/10.1016/j.compgeo.2004.03.004.

Heerten, G., 2007. Improving the Bearing Capacity of Soils with Geosynthetics. 8th International Geotechnical Conference. Bratislava, Slovakia.

Ikeagwuani, C.C. and Nwonu, D.C., 2019. Emerging trends in expansive soil stabilisation: A review. *Journal of Rock Mechanics and Geotechnical Engineering*, 11(2), pp.423–440. https://doi.org/10.1016/j.jrmge.2018.08.013.

Konyushkov, V., Penkov, D. and Fedorenko, E., 2023. Initial data for Hardening Soil model. *E3S Web of Conferences*, [online] 371. https://doi.org/10.1051/e3sconf/202337102019.

Lithuanian Standards Board, 2015. *Unbound and hydraulically bound mixtures - Part 2: Test methods for laboratory reference density and water content - Proctor*.

Lithuanian Standards Board, 2018. *Geotechnical investigation and testing - Laboratory testing of soil - Part 9: Consolidated triaxial compression tests on water saturated soils*.

Lithuanian Standards Board, 2020. *Geotechnical investigation and testing - Identification and classification of soil - Part 2: Principles for a classification*.

Makkar, F.M., 2019. A Review on the Behaviour of Soil against Different Geosynthetic Interfaces. International Conference on Geotechnics for High Speed Corridors. India.

Pacheco, K.W., Matheus, B.C., Pacheco, L.M., Sampa, N.C. and Dienstmann, G., 2021. Analysis of Araquari sand behavior thought numerical modeling of triaxial tests. *XLII Ibero-Latin American Congress on Computational Methods in Engineering*, 3(3).

Palmeira, E.M., 2009. Soil–geosynthetic interaction: Modelling and analysis. *Geotextiles and Geomembranes*, 27(5), pp.368–390. https://doi.org/10.1016/j.geotexmem.2009.03.003.

Pham, D.T., 2023. Application of nonlinear regresssion method to calculate apparent cohesion of geogrid-reinforced soils. *Journal of Science and Technique - Section on Special Construction Engineering*, [online] 6(1). https://doi.org/10.56651/lqdtu.jst.v6.n01.668.sce.

Rathmayer, H.G., Korkiala-Tanttu, L. and Watn, A., 2019. On design principles of reinforced pavement structures - the COST 348 REIPAS action. (2005: Proceedings Seventh International Conference on the Bearing Capacity of Roads, Railways and Airfields), p.10.

Rebolledo, J.F.R., León, R.F.P. and Camapum De Carvalho, J., 2019. Obtaining the Mechanical Parameters for the Hardening Soil Model of Tropical Soils in the City of Brasília. *Soils and Rocks*, 42(1), pp.61–74. https://doi.org/10.28927/SR.421061.

Skuodis, Š., Dirgėlienė, N. and Medzvieckas, J., 2020. Using Triaxial Tests to Determine the Shearing Strength of Geogrid-Reinforced Sand. *Studia Geotechnica et Mechanica*, 42(4), pp.341–354. https://doi.org/10.2478/sgem-2020-0005.

Zakarka, M., 2022. Analysis of the traffic load–induced stresses of embankment. *Mokslas - Lietuvos ateitis*, 14(0), pp.1–7. https://doi.org/10.3846/mla.2022.15179.

Zakarka, M., 2025. *Investigation of soil reinforced with geogrid: mechanical properties and development of their evaluation model*. [online] Vilniaus Gedimino technikos universitetas. Available at: <https://gs.elaba.lt/object/elaba:220641680/>.

Zakarka, M. and Skuodis, Š., 2024. Analysis of Soil-Geogrid Interaction and Alternative Soil Layer Approach for Improved Road Embankment Stability. In: J.A.O. Barros, G. Kaklauskas and E.K. Zavadskas, eds. *Modern Building Materials, Structures and Techniques*, Lecture Notes in Civil Engineering. [online] Cham: Springer Nature Switzerland. pp.643–649. https://doi.org/10.1007/978-3-031-44603-0_66.

Zakarka, M., Skuodis, Š. and Dirgėlienė, N., 2023. Triaxial Test of Coarse-Grained Soils Reinforced with One Layer of Geogrid. *Applied Sciences*, 13(22), p.12480. https://doi.org/10.3390/app132212480.

Zornberg, J.G., 2017. Functions and Applications of Geosynthetics In Roadways. *Procedia Engineering*, 189, pp.298–306. https://doi.org/10.1016/j.proeng.2017.05.048.